



## ORIGINAL ARTICLE

# A 20-kb lineage-specific genomic region tames virulence in pathogenic amphidiploid *Verticillium longisporum*

Rebekka Harting<sup>1</sup> | Jessica Starke<sup>1</sup> | Harald Kusch<sup>1</sup> | Stefanie Pöggeler<sup>2</sup> | Isabel Maurus<sup>1</sup> | Rabea Schlüter<sup>3</sup> | Manuel Landesfeind<sup>4</sup> | Ingo Bulla<sup>5</sup> | Minou Nowrousian<sup>6</sup> | Ronnie de Jonge<sup>7,8</sup> | Gertrud Stahlhut<sup>2</sup> | Katharina J. Hoff<sup>5,9</sup> | Kathrin P. Aßhauer<sup>4</sup> | Andrea Thürmer<sup>10</sup> | Mario Stanke<sup>5,9</sup> | Rolf Daniel<sup>10</sup> | Burkhard Morgenstern<sup>4</sup> | Bart P. H. J. Thomma <sup>8</sup> | James W. Kronstad<sup>11</sup> | Susanna A. Braus-Stromeier<sup>1</sup> | Gerhard H. Braus <sup>1</sup>

<sup>1</sup>Department of Molecular Microbiology and Genetics, Institute of Microbiology and Genetics and Göttingen Center for Molecular Biosciences, University of Göttingen, Göttingen, Germany

<sup>2</sup>Department of Genetics of Eukaryotic Microorganisms, Institute of Microbiology and Genetics and Göttingen Center for Molecular Biosciences, University of Göttingen, Göttingen, Germany

<sup>3</sup>Imaging Center of the Department of Biology, University of Greifswald, Greifswald, Germany

<sup>4</sup>Department of Bioinformatics, Institute of Microbiology and Genetics and Göttingen Center for Molecular Biosciences, University of Göttingen, Göttingen, Germany

<sup>5</sup>Institute for Mathematics and Computer Science, University of Greifswald, Greifswald, Germany

<sup>6</sup>Department of Molecular and Cellular Botany, Ruhr-Universität Bochum, Bochum, Germany

<sup>7</sup>Plant-Microbe Interactions, Department of Biology, Science4Life, Utrecht University, Utrecht, Netherlands

<sup>8</sup>Laboratory of Phytopathology, Wageningen University, Wageningen, Netherlands

<sup>9</sup>Center for Functional Genomics of Microbes, University of Greifswald, Greifswald, Germany

<sup>10</sup>Department of Genomic and Applied Microbiology, Institute of Microbiology and Genetics and Göttingen Center for Molecular Biosciences, University of Göttingen, Göttingen, Germany

<sup>11</sup>Michael Smith Laboratories, Department of Microbiology and Immunology, University of British Columbia, Vancouver, BC, Canada

**Correspondence**

Gerhard H. Braus, Department of Molecular Microbiology and Genetics, Institute of Microbiology and Genetics and Göttingen Center for Molecular Biosciences, University of Göttingen, Grisebachstr. 8, 37077 Göttingen, Germany.  
Email: gbraus@gwdg.de

**Funding information**

Bundesministerium für Bildung und Forschung: BioFung; Natural Sciences and Engineering Research Council of Canada: CREATE; Deutsche Forschungsgemeinschaft, Grant/Award Number: BR1502-15-1, IRTG 2172 and NO407/5-1

**Abstract**

Amphidiploid fungal *Verticillium longisporum* strains VI43 and VI32 colonize the plant host *Brassica napus* but differ in their ability to cause disease symptoms. These strains represent two *V. longisporum* lineages derived from different hybridization events of haploid parental *Verticillium* strains. VI32 and VI43 carry same-sex mating-type genes derived from both parental lineages. VI32 and VI43 similarly colonize and penetrate plant roots, but asymptomatic VI32 proliferation in planta is lower than virulent VI43. The highly conserved VI43 and VI32 genomes include less than 1% unique genes, and the karyotypes of 15 or 16 chromosomes display changed genetic synteny due to substantial genomic reshuffling. A 20 kb VI43 lineage-specific (LS) region apparently originating from the *Verticillium dahliae*-related ancestor is specific for symptomatic

Rebekka Harting and Jessica Starke contributed equally to this work.

This is an open access article under the terms of the Creative Commons Attribution-NonCommercial-NoDerivs License, which permits use and distribution in any medium, provided the original work is properly cited, the use is non-commercial and no modifications or adaptations are made.

© 2021 The Authors. *Molecular Plant Pathology* published by British Society for Plant Pathology and John Wiley & Sons Ltd

VI43 and encodes seven genes, including two putative transcription factors. Either partial or complete deletion of this LS region in VI43 did not reduce virulence but led to induction of even more severe disease symptoms in rapeseed. This suggests that the LS insertion in the genome of symptomatic *V. longisporum* VI43 mediates virulence-reducing functions, limits damage on the host plant, and therefore tames VI43 from being even more virulent.

#### KEYWORDS

genome comparison, hybridization, lineage-specific region, pathogenicity, *Verticillium longisporum*

## 1 | INTRODUCTION

Plant–fungus interactions are dynamic and require ongoing adaptations of both partners to changing conditions in a coevolutionary process. Fungal success requires a balanced equilibrium with the host's immune system, which limits propagation of the invading fungus and restricts plant damage. Analyses of fungal genomes revealed diverse adaptation mechanisms to new ecological niches and different hosts by changes or additions of genetic information (Seidl & Thomma, 2014).

One mechanism representing evolution-driven genome extension in fungi is genome hybridization. Yeast hybrids have often lost complete or large parts of chromosomes, whereas other genomic regions became homozygous (Morales & Dujon, 2012). Ribosomal and mitochondrial DNA become homogenized and mostly derive from one of the two hybridized species (Morales & Dujon, 2012). Retention of duplicated genes presumably depends on the complexity of the genetic interactions between paralogs. A low degree of entanglement favours diversification of the two genes, which then fulfil different functions and persist (Kuzmin et al., 2020). The evolution of filamentous fungal allodiploids by hybridization contributes to the phenotype diversity of human pathogens such as *Aspergillus lactus* (Steenwyk et al., 2020) and plant pathogens such as *Zymoseptoria pseudotritici* (Stukenbrock et al., 2012) or *Verticillium longisporum* (Inderbitzin, Davis, et al., 2011).

Ascomycetous fungi of the genus *Verticillium* are worldwide distributed vascular plant pathogens. Allodiploid *V. longisporum* is the only known interspecific hybrid of its genus, with *V. dahliae* and *V. alfalfae* (formerly *V. albo-atrum*) as its closest relatives (Clewes et al., 2008; Inderbitzin et al., 2013). At least three separate hybridization events between two distinct haploid parental lineages resulted in this species (Inderbitzin, Davis, et al., 2011; Figure 1a). All known *V. longisporum* lineages evolved from the ancestor A1 (not yet isolated), which hybridized with one of three different partners designated D1 to D3. The D2 and D3 strains are classified as *V. dahliae*, whereas D1 represents another not yet identified ancestor. *V. longisporum* lineages A1/D1 and A1/D3 were isolated in Europe, Japan, and the USA, whereas A1/D2 was exclusively found in the USA (Depotter, Rodriguez-Moreno,

et al., 2017; Tran et al., 2013; Zeise & von Tiedemann, 2002). The three hybrids display differences in pathogenicity and are mainly virulent on Brassicaceae (Eynck et al., 2007; Novakazi et al., 2015; Zeise & von Tiedemann, 2002). Lineage A1/D1 is the most pathogenic, whereas lineage A1/D3 is the least able to cause disease on rapeseed.

In contrast to the narrow host range of *V. longisporum*, the relative haploid *V. dahliae* is the main causative agent of *Verticillium* wilt in about 400 different hosts and generates severe yield losses in important crops (EFSA Panel on Plant Health, 2014). Single *V. dahliae* isolates show altered aggressiveness on different hosts and can colonize plants asymptotically (Gibriel et al., 2019; Pegg & Brady, 2002; Resende et al., 1994; Zeise & von Tiedemann, 2002). *V. dahliae* isolates rarely infect Brassicaceae and, when found, remain in lower parts of symptomless plants (Eynck et al., 2007; Zhou et al., 2006). Currently, lucerne is the only known host of *V. alfalfae* (Inderbitzin, Bostock, et al., 2011). Hybridizations between genetically distinct parental species gave rise to *Verticillium* spp. with altered host range and virulence (Inderbitzin, Davis, et al., 2011).

Interspecific hybrids can emerge from sexual mating or by vegetative hyphal fusions. Genes required for sexual mating are present in the genomes of *Verticillium* spp., but sexual reproduction has not yet been observed (Milgroom et al., 2014; Short et al., 2014). For sexual compatibility, opposite idiomorphs of the *MAT* locus, the major regulators of sexual recombination in ascomycetes, are required (Debuchy & Turgeon, 2006; Metzberg & Glass, 1990; Turgeon & Yoder, 2000). Most *V. longisporum* genomes harbour copies of the *MAT1-1* idiomorph, with *MAT1-1-1* and *MAT1-1-3* encoding an  $\alpha$ -box transcription factor and an HMG domain protein (Depotter, Seidl, et al., 2017; Inderbitzin, Bostock, et al., 2011). In contrast, 99% of analysed *V. dahliae* isolates harbour the *MAT1-2* gene (Short et al., 2014). The unequal distribution of the *MAT* idiomorphs and the absence of a sexual cycle suggest that sexual reproduction between the two parental species of *V. longisporum* is unlikely. Extensive sequence changes in the *MAT* loci and separation of genetic clusters in population structure analysis also suggest that sexual reproduction in *V. longisporum* is unlikely (Depotter, Seidl, et al., 2017). Another hybridization mechanism is reproduction by hyphal anastomosis followed by nuclear fusion, resulting in duplication of the genome

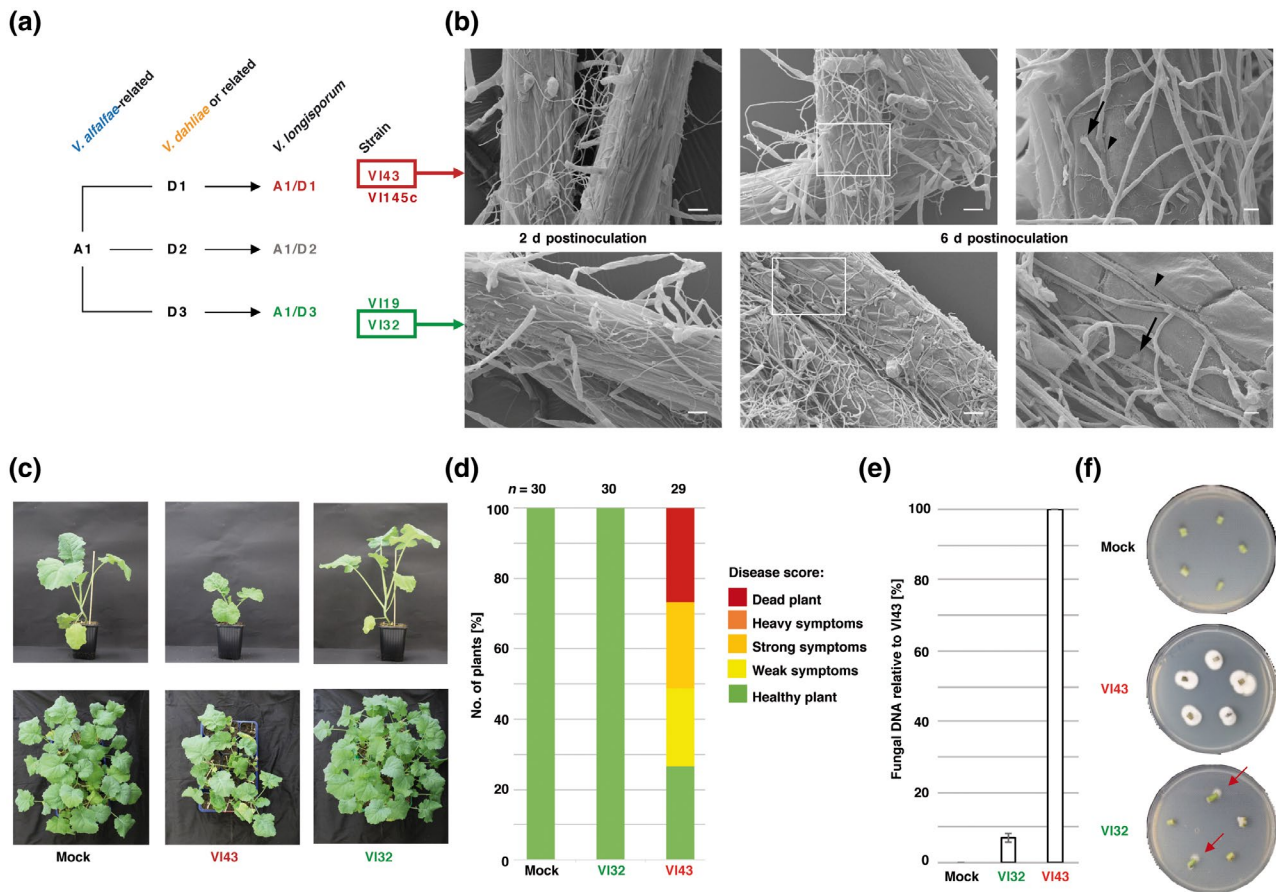


**FIGURE 1** *Verticillium longisporum* VI43 and VI32 colonize *Arabidopsis thaliana* roots, but only VI43 induces disease symptoms in rapeseed. (a) Three allodiploid *V. longisporum* lineages emerged from hybridization events of haploid strains. VI43/VI145c and VI32/VI119 strains originate from hybridization between strains A1 and D1 or D3, respectively (Inderbitzin, Davis, et al., 2011; Tran et al., 2013). (b) Scanning electron micrographs of *V. longisporum* VI32 or VI43 colonizing *A. thaliana* roots 2 or 6 days after root dipping into spore solutions. Scale bars: left and middle, 20  $\mu$ m; right, detailed view of the framed area, 4  $\mu$ m; arrows: hyphopodia as possible entry sites; arrow heads: hyphae growing at interface of plant cells. (c) and (d) *V. longisporum* strain VI43, but not VI32, induces disease symptoms in *Brassic napus*. Plants were evaluated at 35 days postinoculation (dpi) by root dipping into respective spore solutions or water (Mock). (c) Representative plants (above) and overview pictures from a single experiment (below) are shown. (d) The diagram displays the number of plants with indicated symptoms relative to the total number of plants (n) assessed in two independent experiments. (e) *Verticillium* DNA in rapeseed hypocotyl was quantified at 35 dpi with respective spore solutions or water (Mock). *Verticillium*-specific ribosomal DNA was detected by quantitative PCR. Values relative to VI43 are shown as percentages. (f) Reisolation of VI43 and VI32 from surface-sterilized stem slices of infected plants on potato dextrose agar with chloramphenicol after incubation at 25 °C for 7 days was possible. Less outgrowth was detected for VI32 (red arrows)

(Depotter et al., 2016; Karapapa et al., 1997). So far, interspecific vegetative hyphal fusions of haploid *Verticillium* spp. have only been observed for auxotrophic mutants under selection (Hastie, 1973, 1989).

The adaptive evolution of fungal pathogens results in two-speed genomes with a conserved core and a more flexible pan-genome encoding genes required for infection (Dong et al., 2015), such as effectors supporting host colonization by immune response suppression or manipulation of the host's cell physiology as virulence factors (Faino et al., 2016; Gibriel et al., 2019; de Jonge et al., 2013; Kombrink et al., 2017; Selin et al., 2016; Stergiopoulos & de Wit, 2009). The organization of the pan-genome can have different forms. Some fungi carry entire lineage-specific (LS) chromosomes with pathogenicity-related genes (Galazka & Freitag, 2014).

Another nature of karyotype variation was observed in *Verticillium* spp., which display differences in length of chromosomes with rearranged sequence synteny (Faino et al., 2016; de Jonge et al., 2013; Shi-Kunne et al., 2018). A correlation between these chromosomal synteny interruptions, an enrichment of repetitive sequences, and the occurrence of LS regions, which are specific for single isolates or subgroups of strains or species, was observed in *V. dahliae* (de Jonge et al., 2013). Repetitive sequences contribute to centromere diversity and evolution in *Verticillium* (Seidl et al., 2020) and the relative number of genes for niche adaptation is enriched in LS regions compared to the core genome (Gibriel et al., 2019; de Jonge et al., 2013). A correlation of repeat-rich genomic regions and genes for niche adaptations was also observed in other plant pathogens, such as *Leptosphaeria maculans* (Rouxel et al., 2011).

Some *V. dahliae* LS regions were acquired through horizontal gene transfer from *Fusarium oxysporum* (Chen et al., 2018), from plants (de Jonge et al., 2012), or by transposon-mediated processes (Faino et al., 2016; Klosterman et al., 2011). LS regions show higher coding and noncoding sequence conservation compared to the core genome, possibly caused by differences in chromatin organization rather than by horizontal gene transfer (Depotter et al., 2019).

We compared the genomes of the virulent VI43 (A1/D1) and the asymptomatic VI32 (A1/D3) *V. longisporum* strains, which were both isolated from rapeseed in the same area in northern Germany (Zeise & von Tiedemann, 2002). It was evaluated whether the original hybridizations were the result of sexual mating or vegetative hyphal fusions. The contributions of the parental strains to the genetic setup of both hybrids were analysed. Intriguingly, deletion of an LS region, which was only present in pathogenic VI43, did not reduce disease symptom induction, but instead increased the virulence of the pathogenic strain. This unexpected result supports that the corresponding genes, encoding presumed transcription factors, provide functions to reduce disease symptoms and restrict damage in the host plant.

## 2 | RESULTS

### 2.1 | Symptomatic and asymptomatic *V. longisporum* isolates VI43 and VI32 exhibit similar root colonization behaviour

*V. longisporum* VI43 and VI32 were isolated from rapeseed fields in the same area in Germany. VI43 can be highly virulent, whereas plants infected with VI32 did not show significant differences compared to water controls (Zeise & von Tiedemann, 2002). Each amphidiploid strain derived from a different hybridization event of haploid parental strains (Figure 1a). The infection and colonization phenotypes of both strains were compared (Figure 1). Fungal colonization of plant roots represents the first contact followed by penetration into the host. Comparison of VI32 and VI43 growth behaviour on *Arabidopsis thaliana* roots showed similar surface colonization (Figure 1b). Both strains formed hyphae growing along the interface of two plant cells. Thickening of hyphae suggested formation of invasion structures.

Only VI43 induced visible disease symptoms in rapeseed (Figure 1c,d). At 35 days postinoculation (dpi) with VI43 spores 27% of the plants had died. The remaining plants showed strong (30%), weak (27%), or no disease symptoms (17%), whereas all VI32-treated plants appeared mock-like. Amounts of fungal rDNA in hypocotyls of surviving plants dropped more than 10-fold after VI32 compared to VI43 infection (Figure 1e). Both *V. longisporum* strains could be reisolated from stems of infected plants with strong fungal outgrowth of VI43 and lesser growth of VI32 (Figure 1f), suggesting that both isolates are able to colonize the plant's central cylinder, but VI32 to a smaller extent.

It was examined whether the pathotype is connected to differences in the ex planta phenotypes of the strains. Four *V. longisporum* strains were tested on different media, including two strains of the lineages A1/D1 (VI43, VI145c) and A1/D3 (VI32, VI19), as well as *V. dahliae* (VdJR2, Vd39), *V. alfalfae* (Va2), and *V. nonalfalfae* (Va4) strains. All strains could grow on standard media and media with sorbitol or sodium dodecyl sulphate (SDS) as stressors (Figure S1). Individual strains displayed growth and melanization differences, but no clear correlation between phylogenetic lineage and phenotypes under these conditions. A1/D3 strains showed fluffier growth in comparison to A1/D1 strains on malt extract agar (Figure S2). Thick hyphal cables covered VI32 and VI19 colonies, but were rarely observed for A1/D1 strains. Scanning electron microscopy resolved these cables as bundles of single hyphae.

Overall, the ex planta phenotypes of isolates from symptomatic and asymptomatic *V. longisporum* lineages were similar with the exception that asymptomatic strains provide the potential for hyphal cable formation under specific conditions. Root surface colonization behaviour of VI43 and VI32 is similar, but further plant colonization is different and results in distinct pathogenic consequences for the host upon infection with VI43.

### 2.2 | VI32 and VI43 carry same-sex mating-type genes derived from both parental lineages and form vegetative hyphal fusions

Whole-genome sequencing of *V. longisporum* VI43 and VI32 was performed to dissect the genetic basis for the different infection phenotypes. The hybrid *V. longisporum* genome is expected to contain twice the amount of DNA (c.66 Mb) compared to haploid *Verticillium* species (*V. dahliae*: c.36 Mb, Faino et al., 2015; *V. alfalfae*: c.30 Mb, Klosterman et al., 2011) and two copies for the majority of genomic loci (Clewes et al., 2008; Inderbitzin, Davis, et al., 2011; Tran et al., 2013). Previous *V. longisporum* sequencing data (VL1, VL2, VL20, VLB2) suggested a genome size of c.70 Mb (Depotter, Seidl, et al., 2017; Fogelqvist et al., 2018).

A high similarity between loci from the parental genomes makes the assembly of loci within their correct genomic environment challenging. Highly similar regions lead to fragmented assemblies, especially with short sequence reads. First VI43 genome assemblies based on a combination of 454 and paired-read Illumina/Solexa data (Nowrousian et al., 2010) resulted in a total size of the expected c.70 Mb, but a high degree of fragmentation. Three libraries of long jumping distance (LJD) reads were sequenced to improve the assembly continuity (Table S1). Velvet assembly of the combined data (Zerbino & Birney, 2008) resulted in c.75 Mb with an N50 of 1,750 kb, but still a high number of assembly gaps, indicating great improvement of long-range continuity but internal regions of high similarity could not be resolved. A similar strategy based on 454 paired-end and LJD reads was used for the VI32 genome assembly, resulting in c.69 Mb. While having a smaller N50 than the VI43 assembly due to the use of only one LJD library, there are many fewer internal gaps, indicating fewer problems with highly



similar regions. Additionally, a draft genome assembly of pathogenic A1/D1 strain VI145c was generated based on one Illumina/Solexa paired-end library (Tables S2 and S3).

The sexual pathway genes of VI32 and VI43 genomes were compared to address the hybridization origins between the two *Verticillium* lineages. Key functions include genes for potential receptors, pheromones, and mating-type. Two pheromone classes are involved in the sexual reproduction of filamentous ascomycetes: the *Saccharomyces cerevisiae* Pre-Pro-alpha factor-like peptide pheromone precursors and pheromones similar to yeast Mfa lipopeptide pheromone (Coppin et al., 2005; Kim & Borkovich, 2006; Mayrhofer et al., 2006; Pöggeler, 2011). The VI43 genome includes two alleles encoding lipopeptide receptors (*PRE1-1*, *PRE1-2*) and peptide receptors (*PRE2-1*, *PRE2-2*), and two alleles encoding Ppg1-like peptide pheromone precursors (*PPG1-1*, *PPG1-2*, Figure S3a, sequences in Methods S1). The *Verticillium* lipopeptide pheromone differs from typical Ppg2 precursors in Sordariaceae. *Verticillium* Ppg2 resembles the hybrid-type pheromone precursors identified in the order Hypocreales (Schmoll et al., 2010), as it has the Ppg2-typical C-terminal CaaX motif, but it contains five repeats of a dodecapeptide sequence usually found in Ppg1 precursors (Figure S3b). Ppg2-like precursors of *Verticillium* lack a signal sequence and are, presumably, secreted by nonclassical STE6-mediated secretion (Figure S3c).

Typical mating-type (*MAT*) loci of heterothallic mating partners among filamentous ascomycetes consist of dissimilar *MAT1-1* and *MAT1-2* idiomorphs (Turgeon & Yoder, 2000). *MAT1-1* invariably contains the *MAT1-1-1* gene encoding an  $\alpha$ -box domain protein. The *MAT1-2* locus carries *MAT1-2-1* encoding a protein with an HMG DNA-binding domain (Debuchy et al., 2010). Both mating-type loci can include additional genes: most Sordariomycetes *MAT1-1-2* loci encode a protein with a PPF (proline/proline/phenylalanine) domain, or *MAT1-1-3* encodes another HMG domain DNA-binding protein. Genomes of self-fertile (homothallic) filamentous ascomycetes contain either linked or unlinked genes indicative of both mating-types (Debuchy & Turgeon, 2006; Pöggeler, 2001).

*V. longisporum* isolates VI43, VI32, and VI145c each contain two *MAT1-1* alleles (Inderbitzin, Davis, et al., 2011). BLAST searches failed to detect *MAT1-2* homologs. The VI43 genome assembly was not sufficiently complete to determine whether the arrangement of the mating-type genes of the *V. longisporum* *MAT1-1* idiomorphs is similar to the *MAT1-1* idiomorphs of *V. dahliae* (D-type) or *V. alfalfae* (A-type) because the mating-type idiomorph flanking gene *SLA2* was distributed on different scaffolds. PCR experiments using VI43 DNA as template and the VI32 assembly revealed that both mating-type loci are flanked by *SLA2* and *APN2*. The idiomorph sequences encode the mating-type genes *MAT1-1-1* and *MAT1-1-3* in a tail-to-tail orientation (Figure 2a, Table S4, and Sequences in Methods S1). VI32 and VI43 *Mat1-1-1* and *Mat1-1-3* proteins display high amino acid sequence identity when compared among the A- or D-types, but a reduced level of amino acid sequence identity when compared between the A- and D-type loci of the same strain. *Mat1-1-1* and *Mat1-1-3* proteins are more similar to *V. dahliae* than to *V. alfalfae* proteins. Mating-type

proteins of the VI32 *MAT1-D* locus are 100% identical to *V. dahliae* *Mat1-1-1* and *Mat1-1-3* (Tables S5 and S6, and Figure 2b). The main sequence differences between A and D loci are in the intergenic region of *MAT1-1-3* and *APN2* genes. The *MAT1-D* locus contains a short 295 bp sequence with high sequence similarity to hypothetical open reading frames (ORFs) located in the *MAT*-flanking regions of *V. dahliae* (VDAG\_06529) and *V. alfalfae* (VDBG\_03574.1) (Figure 2b). In contrast, the intergenic *MAT1-1-3/APN2* region of VI43 and VI32 *MAT-A* loci contains the entire coding region of VDAG\_06529.

*V. longisporum* VI43 and VI32 carry two *MAT1-1* alleles, one from each parent, and miss an opposite *MAT1-2* idiomorph. One *MAT1-1* locus present in both *V. longisporum* isolates contains an ORF homologous to VDAG\_06529 and VDBG\_03574, which is not localized adjacent to the mating-type genes in *V. dahliae* or *V. alfalfae*. This might reflect the genomic situation of the yet unidentified parental strain A1. The finding that both mating alleles in VI43 and VI32 belong to the same idiomorph suggests that VI43 and VI32 are presumably not derived from a mating event or, if hybridization is the result of mating, a homogenization of the initial loci must have happened.

Scanning electron microscopy explored the possibility of same-sex hybridization events. Individual hyphae of *V. longisporum* can be interconnected by anastomoses (Figure 2c). This was frequently observed within the hyphal cables of asymptomatic (VI32, VI19), but rarely in pathogenic (VI43, VI145c) isolates, most often in close contact with the agar surface. It is yet unclear whether same-sex hybridization was the origin of *V. longisporum* because anastomoses could only be observed for hybrid and not for haploid putative parental strains.

### 2.3 | The two *V. longisporum* genomes display minimal gene variations but different numbers of massively rearranged chromosomes

The two parental origins of VI32 and VI43 hybrid genomes were visualized by plotting the relative identity between either of the two *V. longisporum* isolates against *V. dahliae* long DNA contigs (Figure 3a). Both plots display two similarity peaks: one close to 100% identity, resembling the D1/D3 component, the other 94% identity of A1 origin. Plotting of *V. alfalfae* against *V. dahliae* sequences visualizes that *V. dahliae* is approximately as related to *V. alfalfae* as to A1. As control, the plotting of two *V. dahliae* strains, VdLs.17 (Klosterman et al., 2011) and VdJR2 (de Jonge et al., 2012; Faino et al., 2015; Fradin et al., 2009), resulted in almost 100% identity.

*V. longisporum* gene gain or loss after hybridization was addressed by comparing predicted ORFs against the scaffolds of relative *Verticillium* spp. using a BLAST-based clustering approach. The number of genes unique to each *V. longisporum* genome was below 1% (Figure 3b). Analysis of the putative *V. longisporum* strain-specific genes demonstrated that the respective regions are very short (1 to 11 genes).

*V. dahliae* and *V. alfalfae* genomes consist of seven or eight chromosomes, as shown by restriction fragment length polymorphism

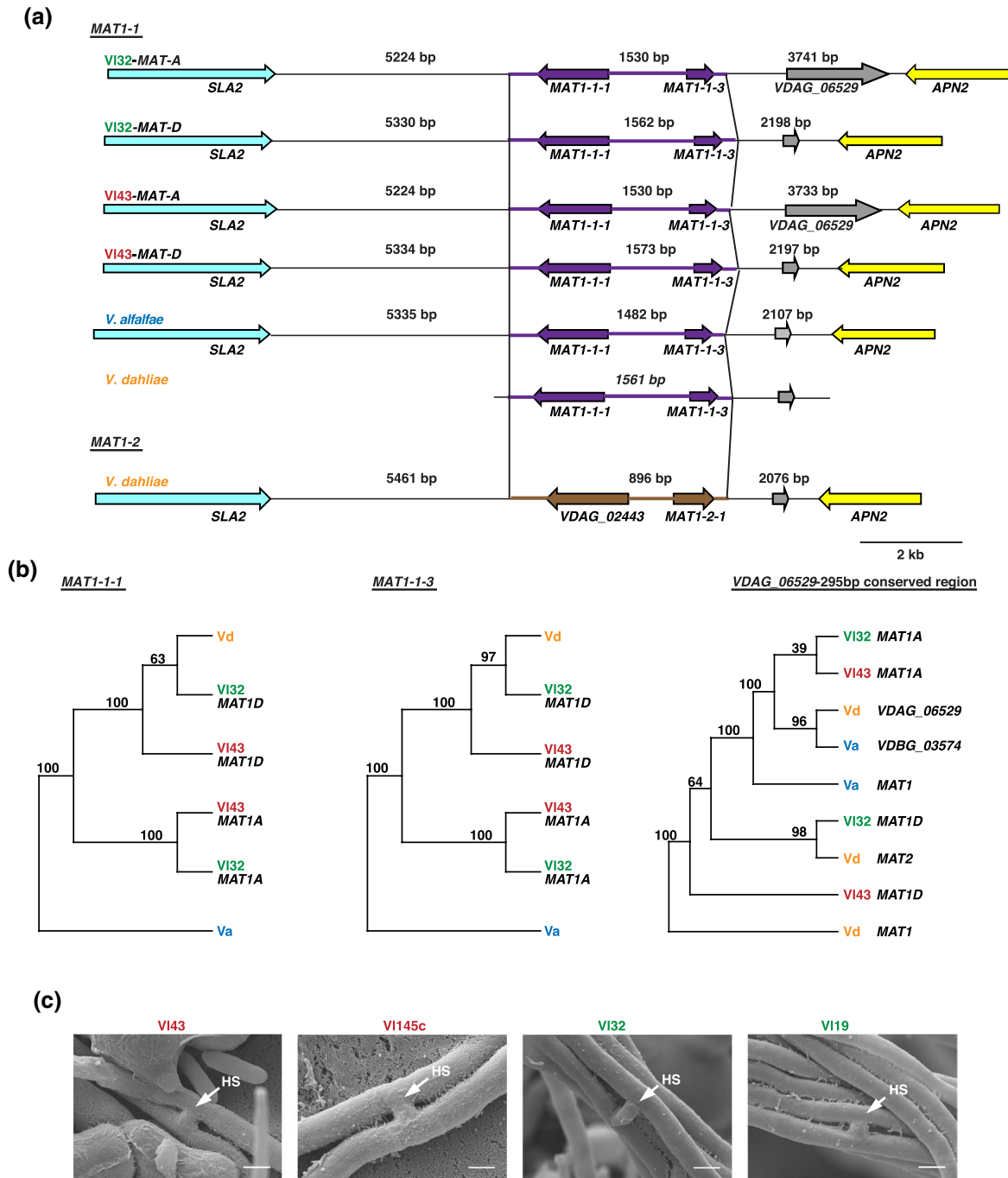


**FIGURE 2** *Verticillium longisporum* VI32 and VI43 harbour same-sex mating-type genes originating from both parental lineages. (a) Comparison of *V. longisporum* VI32 and VI43 MAT1-1 and *V. dahliae* (Vd)/*V. alfalfae* (Va) mating-type loci with flanking regions. Lines: intergenic regions; purple arrows: MAT1-1-specific regions; brown arrows: MAT1-2-specific regions; vertical line: border of the idiomorph sequence. Sequences from Va MAT1-1 and Vd MAT1-2 loci from Ensembl Fungi (Kersey et al., 2018) and Vd MAT1-1 (AB505215.1) were used. (b) Phylogenetic tree of MAT1-1-1, MAT1-1-3, and a conserved 295-bp region of VDAC\_06529 homologs. Consensus trees based on nucleotide sequences were calculated with PHYLIP program NEIGHBOR. Percentages based on 1,000 replications of the neighbour-joining procedure are shown. (c) Scanning electron micrographs of hyphal fusion sites (HS) from *V. longisporum* strains of lineage A1/D1 (VI43, VI145c) or A1/D3 (VI32, VI19) cultivated on malt extract agar for 3 days are shown (scale bar: 2  $\mu$ m)

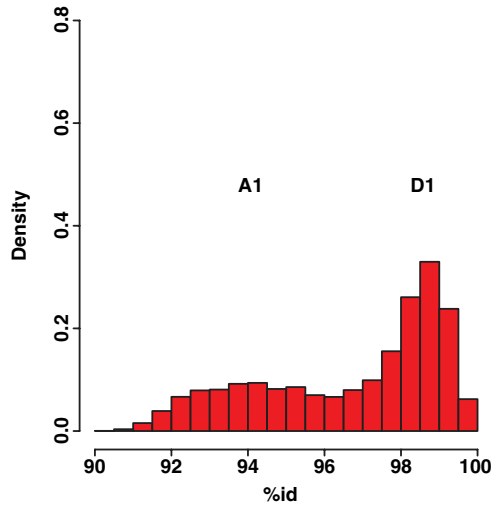
and optical mapping (Faino et al., 2015; Klosterman et al., 2011; Pantou & Typas, 2005). Optical mapping of both genomes revealed that the VI32 genome is distributed among 16 chromosomes, which fits with the genome duplication (Figure 4a). In contrast, the VI43 genome consists of only 15 chromosomes, one less than in VI32.

Comparing chromosome sizes between VI43 and VI32 we concluded that the difference is not only an additional chromosome for VI32, but a difference in length for all chromosomes.

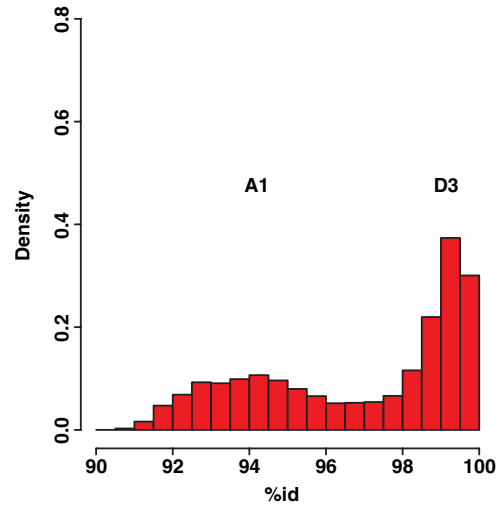
Analysis of syntenic regions between VI43, VI32, and VdLs.17 showed a much larger overlap between VI32 and the *V. dahliae* isolate

(a)

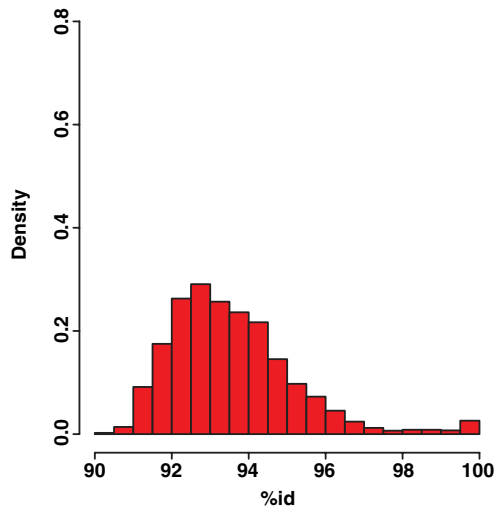
*V. dahliae* vs. VI43



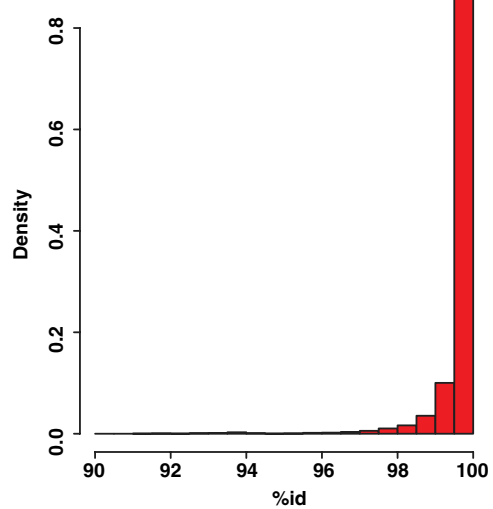
*V. dahliae* vs. VI32



*V. dahliae* vs. *V. alfalfae*



*V. dahliae* vs. *V. dahliae*



(b)

Number of genes specific for

| VI43<br>(21,176 <sup>a</sup> ) | VI32<br>(19,313 <sup>a</sup> ) | <i>V. dahliae</i><br>(10,535 <sup>b</sup> ) | <i>V. alfalfae</i><br>(10,221 <sup>b</sup> ) | versus               |
|--------------------------------|--------------------------------|---------------------------------------------|----------------------------------------------|----------------------|
| -                              | 73                             | 233                                         | 144                                          | VI43                 |
| 149                            | -                              | 227                                         | 180                                          | VI32                 |
| 49                             | 87                             | 216                                         | 146                                          | VI145c               |
| -                              | 69                             | 204                                         | 134                                          | VI43 + VI145c        |
| -                              | -                              | 130                                         | 121                                          | VI43 + VI145c + VI32 |
| 455                            | 386                            | -                                           | 296                                          | <i>V. dahliae</i>    |
| 863                            | 676                            | 585                                         | -                                            | <i>V. alfalfae</i>   |

**FIGURE 3** *Verticillium longisporum* strains are two-parent hybrids. (a) In VI43 and VI32 genomes, two identity groups are bimodally resembled in the distribution of relative identity (%id) of long genomic contig (>1,000 kb) alignments. Contigs of VI43, VI32, VaMs.102, and VdJR2 were compared to the VdLs.17 genome using Exonerate software (Slater & Birney, 2005). (b) Strain-specific genes in *Verticillium* genomes. Numbers given in the top row represent the total amount of predicted open reading frames (ORFs). VdLs.17 and VaMs.102 were used as *V. dahliae* and *V. alfalfae* reference genomes, respectively (Ensembl Fungi; Kersey et al., 2018). Total numbers of predicted ORFs per genome according to Augustus prediction<sup>a</sup> and Klosterman et al. (2011)<sup>b</sup> are given

(14 Mb) than between VI43 and VdLs.17 (<1 Mb) (Figure 4b). VI32 and VI43 shared approximately 26 Mb syntenic regions, whereas only approximately 1 Mb are in synteny between all strains. Collinear blocks of the 15 VI43 and the 16 VI32 chromosomes were visualized (Figure 4c). The high number of lines connecting the syntenic blocks of the respective chromosomes indicates massive syntenic rearrangements. These can correlate to repetitive sequences (Depotter et al., 2016; Faino et al., 2016; Möller & Stukenbrock, 2017; Seidl & Thomma, 2017). In addition, 10% and 12% of the VI32 and VI43 genomes consist of repeats compared to 4% of *V. dahliae* (Table S7). The de novo analysis found repetitive sequences of *V. alfalfae* and *V. dahliae* do not give much more repeat masking than with the general RepeatMasker libraries. In contrast, in the *V. longisporum* strains, de novo analysis found repeats mask a much higher percentage of the genome. Similar to the ascomycete *Pyronema confluens* (Traeger et al., 2013), this indicates a more recent expansion of *V. longisporum* repetitive sequences (Figure S4).

Our comparisons suggest minimal gene gain or loss in the hybrid genomes compared to *V. dahliae* and *V. alfalfae*. The plant colonizer VI32 has 16 chromosomes, whereas the symptom inducer VI43 has only 15. *V. longisporum* genomes are massively rearranged and enriched with repetitive sequences.

## 2.4 | A 20 kb genomic region absent in asymptomatic *V. longisporum* VI32 reduces disease symptom induction in *Brassica napus* by virulent VI43

Comparison of asymptomatic *V. longisporum* VI32 to pathogenic VI43 revealed few specific genes within the two amphidiploid genomes. Genomic rearrangements and evolution of LS regions correlate in haploid *Verticillium* spp. (Chen et al., 2018; de Jonge et al., 2013; Gibriel et al., 2019; Klosterman et al., 2011). Four LS regions (LS1–4) of about 300 kb in the genome of *V. dahliae* VdLs.17 (Faino et al., 2016) share no synteny to the *V. alfalfae* VaMs.102 genome (Klosterman et al., 2011). These four VdLs.17 LS regions with enriched repetitive sequences might increase genetic flexibility for *V. dahliae* to adapt to different host niches. A bioinformatic search for VdLs.17 orthologs present in the VI43 genome was performed to identify candidates important for this *V. longisporum* pathotype. Small LS1, LS3, and LS4 subregions were conserved in synteny in pathogenic A1/D1 *V. longisporum* isolates VI43 and VI145c, as well as in haploid *V. dahliae* JR2 (Figure 5a). This synteny was disrupted in the asymptomatic A1/D3 isolate VI32. The small VI43LS20kb subregion of approximately 20 kb was present in VI43, but absent from the VI32 genome and also from the genome of haploid *V. alfalfae* VaMs.102. The absence of this region in VI32 was verified by

PCR analyses targeting seven genes (LS region gene = LSG1–LSG7, Figure 5b, Table S8) predicted for the VI43LS20kb region (gene annotations according to *V. dahliae* JR2 in Ensembl Fungi; Faino et al., 2015; de Jonge et al., 2012; Kersey et al., 2018). LSG3 and LSG6 code for potential transcription factors. All LSGs are present in single copy in *V. longisporum* VI43 or VI145c. Instead, two copies for LSG1, one not yet annotated (in the VI43LS20kb homologous region between VDAG\_JR2\_Ch2g10300a and VDAG\_JR2\_Ch2g10310a) and a second copy on chromosome 5 (VDAG\_JR2\_Ch5g10950a) are present in the haploid *V. dahliae* JR2 genome.

VI43 deletion strains were examined to determine whether the pathogen-specific VI43LS20kb region encodes pathogenicity factors. The VI43LS20kb region was divided into two subregions (LSI: c.11.5 kb with LSG1–LSG5; LSII: c.8.5 kb with LSG6–LSG7). LSI, LSII, or the total LS region were deleted in VI43 (Figures 5a and S5a,b). VI43ΔLSI, VI43ΔLSII, and VI43ΔLS spot inoculated onto different media with or without stress-inducing agents appeared like the wild type ex planta (Figures 5c and S5c). In rapeseed infection experiments, the VI43ΔLSI, VI43ΔLSII, and VI43ΔLS strains induced more severe disease symptoms after 35 days compared to plants inoculated with wild-type VI43 spores (Figure 5d,e). Also, 27% of the plants inoculated with the wild-type VI43 died from fungal infection, whereas there were 70% dead plants for VI43ΔLSI, 83% for VI43ΔLSII, and 89% for VI43ΔLS. The small amount of surviving plants at the end of the experiment did not allow a quantification of fungal DNA.

The VI43LS20kb region is in the same syntenic arrangement in the pathogenic A1/D1 *V. longisporum* isolate VI145c and in *V. dahliae* JR2. The VI43LS20kb homologous region in *V. dahliae* JR2 was deleted (Figure S6a,b). The ex planta phenotypes of *V. dahliae* JR2ΔLS spot inoculated onto different media revealed that the LS region is dispensable for vegetative growth of *V. dahliae*, as found for *V. longisporum* VI43 (Figure S6c). Tomato plants were inoculated with conidiospores from two independent *V. dahliae* JR2ΔLS transformants. Severity of disease symptoms was unaltered for both wild-type- and JR2ΔLS-treated plants after 21 days (Figure S6d,e). Hypocotyl cross-sections of *V. dahliae* JR2ΔLS-infected plants showed wild-type-like discolouration, indicating no alterations in plant defence responses. The potential of *V. dahliae* JR2ΔLS to induce disease symptoms in rapeseed was tested and revealed wild-type-like absence of disease symptoms in treated plants (Figure S7).

In summary, the VI43LS20kb region of pathogenic *V. longisporum* VI43 fulfils an unexpected function, which differs to the corresponding *V. dahliae* JR2 region. In contrast to the prediction that VI43LS20kb, which is absent in the asymptomatic isolate VI32, contributes to virulence, this region even tames the pathogenic features of VI43 and reduces disease symptom severity induced in rapeseed.



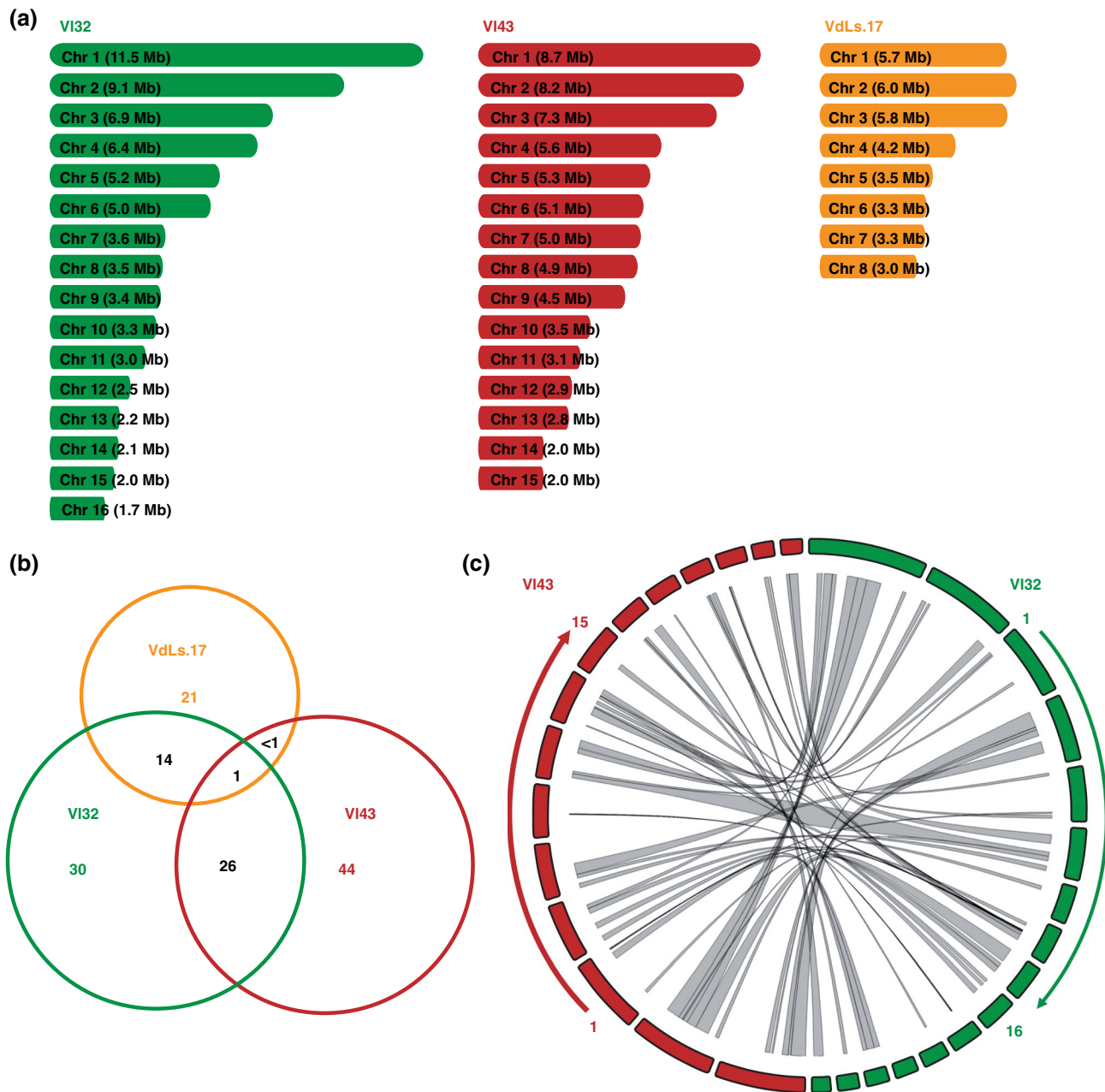


**FIGURE 4** Genome rearrangements between *Verticillium longisporum* VI43 and VI32. Mapping is based on restriction patterns determined by optical mapping (OptGen). (a) Illustration of VI43 and VI32 chromosome numbers and sizes compared to *V. dahliae* VdLs.17 (de Jonge et al., 2013). (b) The Venn diagram illustrates the length (Mb) of overlapping and unique syntenic regions in VI43, VI32, and VdLs.17 genomes. Genome synteny is partially conserved between VI32 and VdLs.17 and between VI32 and VI43. Synteny overlap between VI43 and VdLs.17 is very low. (c) Chromosome synteny comparison in a Circos diagram reveals a high level of genomic rearrangements by illustration of collinear blocks between 15 VI43 (red) and 16 VI32 (green) chromosomes.

This suggests a trade-off strategy in the interaction between a fungus and its host plant, resulting in evolutionary advantages.

### 3 | DISCUSSION

*V. longisporum* VI43 and VI32 are two representatives of interspecies lineages deriving from distinct hybridizations (Inderbitzin, Davis,

et al., 2011). VI43 of lineage A1/D1 causes severe symptoms in rapeseed plants, whereas VI32 of the A1/D3 lineage colonizes plants asymptotically (Depotter, Rodriguez-Moreno, et al., 2017; Zeise & von Tiedemann, 2002). VI43 is also able to cause symptoms in *Arabidopsis thaliana* (Reusche et al., 2012). Both strains colonize roots similarly, but fungal biomass reisolated from infected tissue is higher for VI43 than for VI32. Successful root penetration is performed by both, but they differ in subsequent steps of host plant colonization

resulting in higher amounts of fungal VI43 DNA in hypocotyls of infected plants. This is similar in nonpathogenic compared to pathogenic *F. oxysporum* (Validov et al., 2011). *Verticillium* spp. colonize the host plant's vascular system, which is nutrient-poor and imbalanced in amino acids (Singh et al., 2010). *V. longisporum* recognizes this environment and responds with a highly specific secretion pattern, including pathogenicity-related effectors (Leonard et al., 2020).

The genomes of *V. longisporum* VI43 and VI32 with different pathotypes revealed high gene level conservation, but different chromosome numbers and sizes combined with increases in repetitive sequences. VI32 and VI43 carry genes for potential pheromones and their receptors as well as two *MAT1-1* same-sex mating-type genes derived from both parental strains, but no *MAT1-2*. One of these parental alleles contains an additional complete ORF of unknown

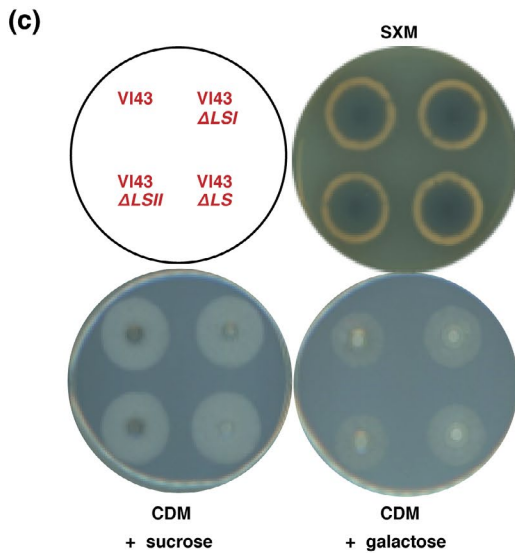
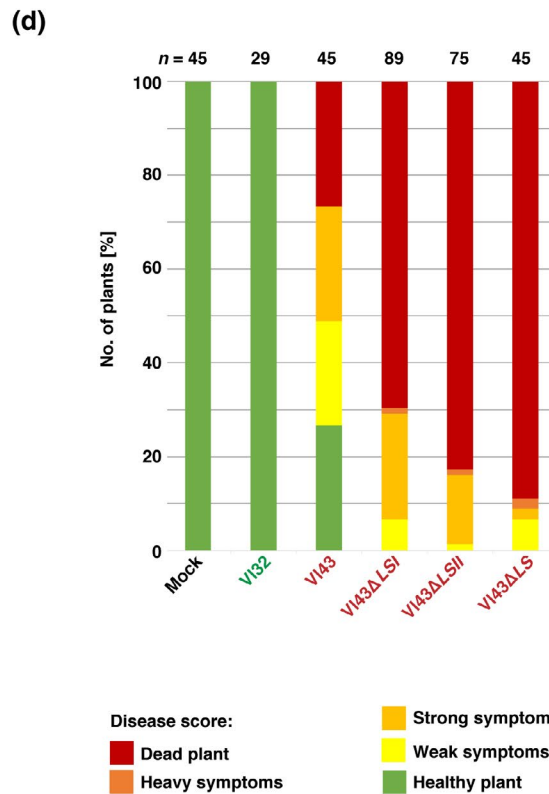
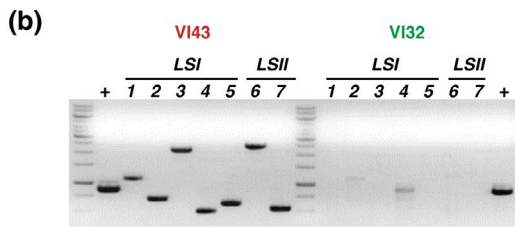
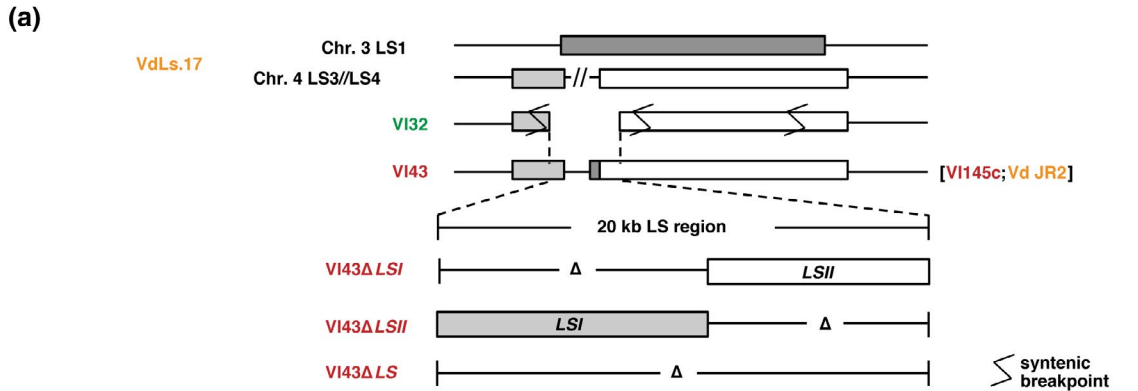


**FIGURE 5** The *VI43LS20kb* region of *Verticillium longisporum* VI43 reduces severity of *Brassica napus* disease symptoms. (a) Arrangement of the 20 kb lineage-specific (LS) region and adjacent regions in pathogenic (red) and asymptomatic (green) *V. longisporum* strains compared to *V. dahliae* VdLs.17 LS regions LS1 (dark grey), 3 (light grey), and 4 (white). Parts of VdLs.17 LS1 located on chromosome 3 as well as parts of LS3 and LS4 regions located on chromosome 4 are in synteny in the genomes of VI43, VI145c, and VdJR2, but disrupted in the VI32 genome at indicated breakpoints. The 20 kb LS region is absent from the VI32 genome. The *VI43LS20kb* region was subdivided into *LSI* and *LSII*. VI43 deletion strains lack *LSI*, *LSII*, or the total 20 kb LS region. (b) Absence of the *VI43LS20kb* region in the VI32 genome was verified. Seven genes (*LSG1*–*LSG7*) were amplified from DNA of VI43, but not of VI32. Histone H2A served as positive control (+). (c) Ex planta phenotypes of *VI43ΔLSI*, *VI43ΔLSII*, *VI43ΔLS* strains on simulated xylem fluid medium (SXM; bottom view) and Czapek Dox medium (CDM) with sucrose or galactose (top view) for 14 days at 25 °C show no significant alterations compared to VI43. (d) and (e) *V. longisporum* *VI43ΔLSI*, *VI43ΔLSII*, and *VI43ΔLS* induce more severe disease symptoms in *B. napus* compared to wild-type VI43 and asymptomatic VI32 35 days postinoculation by root dipping into respective spore solutions or water (Mock). (d) The diagram displays the number of plants with indicated symptoms relative to the total number of plants (*n*) from three experiments with two independent *VI43ΔLSI*, *VI43ΔLSII* transformants and one *VI43ΔLS* transformant. (e) Representative overview pictures of plants from a single experiment

function, which might reflect the genomic situation of the yet unknown A1 strain. If hybridization is based on mating, the initial locus must have been homogenized as found for the rDNA genes (Tran et al., 2013). Because *MAT1-1* loci are rare in haploid *Verticillium* spp., hyphal anastomosis and nuclear fusions are more likely. However, only self-anastomosis of VI43 and VI32 was achieved, which could not be verified with haploid species.

The increased chromosome number in asymptomatic VI32 was not due to an accessory chromosome comprising species-specific genes but arose from rearranged genomic regions. Similarly, frequent synteny breakpoints caused by genomic rearrangements occur in all *Verticillium* spp. (Shi-Kunne et al., 2018). In eukaryotes, chromosomal reshuffling is often linked to phenotypical alterations and gene gains or losses affect fitness levels in different niches (Coghlan et al., 2006; Dong et al., 2015; Plissonneau et al., 2018; Tang & Amon, 2013).

Genomic rearrangements and the evolution of LS regions correlate in haploid *V. dahliae* (Chen et al., 2018; Faino et al., 2016; Gibriel et al., 2019; de Jonge et al., 2013; Klosterman et al., 2011). In *V. dahliae* VdLs.17, host range expansion and niche adaptation compared to *V. alfalfae* might be mediated by LS1–4 regions (Klosterman et al., 2011). Different *V. dahliae* isolates showed increased numbers of effector genes in LS regions when compared to the core genome, although the number of effectors was small relative to the total number of genes encoded in the LS region (Gibriel et al., 2019; de Jonge et al., 2013). Most studies have identified LS regions by comparison of *V. dahliae* isolates. *V. dahliae* and *V. alfalfae* genomes comprise the same relative numbers of genes for secreted proteins in the core and LS regions (Klosterman et al., 2011). Within the flexible regions, transposable elements, gene duplications as well as genes linked to pathotypes, regulation of transcription, signalling, degradation of organic material, and iron or lipid metabolic processes can be found (Klosterman et al., 2011). Some of these might be connected to niche adaptation. LS regions of *V. dahliae* could represent a unique chromatin state with regard to transposable elements, methylation marks, and DNA accessibility when compared to the core genome (Cook et al., 2020).

We discovered that a genomic LS region, originating from the *V. dahliae*-related parental lineage D1, is present in pathogenic isolates VI43 and VI145c, but absent in the genome of the asymptomatic *V. longisporum* isolate VI32. The *VI43LS20kb* homologous region

of *V. dahliae* JR2 seems not to play a role in pathogenicity towards tomato or rapeseed plants. Characterization of the *VI43LS20kb* region in *V. longisporum* VI43 revealed that this region does not contain virulence factors that explain the difference of this pathogenic strain to the asymptomatic VI32. In contrast, this region has a negative impact on disease symptom severity induced in *V. longisporum* VI43-colonized rapeseed plants and tames the fungus in its relationship with the plant. The virulence-suppressing function of the *VI43LS20kb* region keeps VI43 at an intermediate virulence level, which might be beneficial for fungal accumulation within the host plant. It is still unknown whether the genes of this region also affect other *Verticillium* species. The damage response network has been developed as a concept for describing microbial–host interactions ranging from commensalism to colonization to disease. These interactions differ in the degree of damage encountered by the host, which can be caused by the host response, by the microbe, or by the combination of both and make it difficult even within the same species to define what is a host and what is a pathogen (Casadevall & Pirofski, 2014, 2018). In line with this, isolates of the same *V. longisporum* lineage differ in pathogenicity on different host plants (Novakazi et al., 2015). These observations support the idea that different *Verticillium* strains of the same species display a high degree of specialization and adaptation to specific hosts depending on a variety of parameters. The acquisition of new genes might contribute to this specialization but, additionally, existing responses to the environment might be differentially regulated. The ex planta phenotypes of LS deletion strains resembled the wild-type VI43, suggesting that the induction of more severe symptoms in planta and the detrimental impact on the host is not connected to increased fungal growth or propagation.

Gene losses due to chromosomal rearrangements can play significant roles in niche adaptation in various plant-colonizing fungi (Hartmann et al., 2017; Plissonneau et al., 2018; Sharma et al., 2014). Deletion of the *VI43LS20kb* region might result in misregulation of virulence factors or virulence-attenuating factors. Consistently, the pathogenic isolate is less tolerable for rapeseed plants when the *VI43LS20kb* region is absent. These virulence or virulence-attenuating factors might not be present or expressed in the asymptomatic colonizer VI32.

Asymptomatic or less virulent isolates might contain pathogenicity-related genes in their genomes that are active or inactive depending on differences in the control of various transcriptional

networks. The *VI43LS20kb* region identified in the pathogenic *VI43* strain encodes two potential transcription factors. Both proteins are candidates for the regulation of virulence-associated genes. Transcriptional control of virulence-related genes has been observed during analysis of related fungal species with different pathotypes. Transcriptome analyses of *V. dahliae* isolates with different potential to induce disease symptoms in cotton revealed decreased transcript levels of genes for virulence-connected proteins. Potential transcription factors for pathogenicity-related gene control were enriched in the less virulent strain (Jin et al., 2019). *V. dahliae* *Vta2*, *Vta3*, *Som1*, and *Sge1* transcription factors control pathogenicity and development (Bui et al., 2019; Santhanam & Thomma, 2013; Tran et al., 2014). Transcription factors with negative impact on virulence include the pH-dependent regulator *PacC* of *F. oxysporum* for repression of low pH-expressed genes. *PacC* mutants are more virulent on tomato plants (Caracuel et al., 2003). *Alternaria brassicicola* *Amr1* represses hydrolytic enzyme transcription (Cho et al., 2012). In other plant pathogens *Amr1* regulates melanin biosynthesis, which is not necessarily linked to virulence in *V. dahliae* (Harting et al., 2020; Wang et al., 2018).

To our knowledge, this is the first study describing an LS region that decreases the virulence of a pathogenic *Verticillium* isolate. The asymptomatic isolate *VI32* lacks this region. Besides the addition or loss of genes coding for pathogenicity factors, regions required for pathogenicity attenuation contribute to the formation of different pathotypes. These regions and the encoded functions may help closely related strains to control the degree of damage in a specific host and in a defined environmental context.

## 4 | EXPERIMENTAL PROCEDURES

Strains, primers, and plasmids are listed in Tables S10–S12. Cultivation conditions, strain constructions, plant experiments, and phylogenetic analyses are described in Methods S1. Fungal transformants were verified by Southern hybridization (Bui et al., 2019).

### 4.1 | DNA preparation and sequencing strategy

Fungal genomic DNA for Southern hybridization and whole-genome sequencing was isolated from mycelium grown in potato dextrose broth (Carl Roth) for 1 week at 25 °C. Mycelium was harvested with Miracloth (Calbiochem Merck), rinsed, tissue-dried, ground in liquid nitrogen, and genomic DNA was isolated (Kolar et al., 1988). A single-stranded DNA shotgun library (ssDNA library) was generated from approximately 5 µg genomic DNA. DNA was fragmented by nebulization for 30 s at 1 bar. Further steps were done according to the Roche protocol. Sequencing was done using the Genome Sequencer FLX system (Roche Applied Science). Illumina sequencing was performed by GATC Services (Eurofins Genomics) using the Genome Analyzer SN365-Hi-Seq2000 with the TruSeq SBS v. 5 kit (Illumina). Sequenced libraries were processed using a sequence length cut-off

of 30 bp for paired sequences as well as for shotgun sequences. The input data for the assemblies can be found in Table S1.

### 4.2 | Assembly and k-mer frequency analysis

Before assembly, 454 and Illumina raw data were trimmed with custom-made Perl scripts as described (Nowrousian et al., 2012; Teichert et al., 2012). Details on assembly generation can be found in Methods S1. *k*-mer frequencies were analysed as described previously (Potato Genome Sequencing Consortium, 2011; Traeger et al., 2013) (Table S9 and Figure S8). Illumina/Solexa read pairs from paired-end libraries after trimming were used for the analysis.

### 4.3 | Genome annotation

Structures of *VI43* and *VI32* protein-coding genes were annotated with AUGUSTUS (Stanke et al., 2008), which was trained for *V. longisporum*. Learned parameters and evidence from the repeat masked genomes, homolog proteins, RNA-Seq, and EST data, and peptide sequences were used for gene prediction in the two genome assemblies (see Methods S1). In *VI43* and *VI32* genome assemblies 21,176 and 19,313 protein-coding genes were found, respectively. The median number of coding exons per gene was three for both genomes. The number of strain-specific genes was determined by a BLAST-based clustering approach using the predicted ORFs of *V. longisporum* *VI32* and *VI43*, *V. dahliae* *VdLs.17*, and *V. alfalfae* *VaMs.102* (Ensembl Fungi, <http://fungi.ensembl.org/>; Kersey et al., 2018).

### 4.4 | Repeat content analyses

Transposable elements and other repeats were analysed with RepeatMasker (A.F.A. Smit, R. Hubley, P. Green; RepeatMasker Open; [www.repeatmasker.org](http://www.repeatmasker.org)) based on the RepbaseUpdate library (Jurka et al., 2005) and a library of de novo-identified repeat consensus sequences that was generated by RepeatModeler (A.F.A. Smit, R. Hubley; RepeatModeler Open; [www.repeatmasker.org](http://www.repeatmasker.org)). Details can be found in Methods S1.

### 4.5 | Whole-genome comparison and visualization of collinear blocks

Optical maps of *VI32* and *VI43* were generated and visualized by OpGen using the Mapsolver software (OpGen).

### 4.6 | Sequence analyses

As reference genomes the following sequences in the Ensembl Fungi genome database (Kersey et al., 2018) were used: *V. dahliae* *VdLs.17*



(Klosterman et al., 2011) and JR2 (de Jonge et al., 2012), *V. alfalfae* VaMs.102 (Klosterman et al., 2011).

Conserved domains were predicted with the InterPro webpage (<http://www.ebi.ac.uk/interpro/>; Mitchell et al., 2019). Protein localization was analysed using DeepLoc 1.0 (<http://www.cbs.dtu.dk/services/DeepLoc/>; Almagro Armenteros et al., 2017). Nuclear localization sites were predicted by cNLS-Mapper ([http://nls-mapper.iab.keio.ac.jp/cgi-bin/NLS\\_Mapper\\_form.cgi](http://nls-mapper.iab.keio.ac.jp/cgi-bin/NLS_Mapper_form.cgi); Kosugi et al., 2009).

#### 4.7 | Presence/absence verification of LS regions and analyses of MAT loci

The LS region and the VI43 MAT locus were amplified by PCR from genomic DNA. For details see Methods S1.

#### 4.8 | Light and electron microscopy

A binocular microscope (Olympus) with cellSens dimension software (v. 1.4; Olympus) was used for light microscopy of colonies, hyphae, and stem tissue. For details on electron microscopy see Methods S1.

#### ACKNOWLEDGEMENTS

The authors thank Nicole Scheiter, Anne Reinhard, and Stefan Bock for excellent technical assistance, Clara Hoppenau, Kai Nesemann, and Christian Timpner for genomic DNA, Luigi Faino for PacBio annotation support, Andreas von Tiedemann, Derek Barbara, and Riccardo Baroncelli for *V. longisporum* strains, the Norddeutsche Pflanzenzucht for *B. napus* seeds, and Miriam Leonard, Annalena Höfer, and Alexandra Nagel for support. J.S. and I.M. were supported by IRTG 2172 PRoTECT and CREATE (co-directed by J.W.K.) from the Natural Sciences and Engineering Research Council of Canada. Funding was provided by DFG grant BR1502-15-1 and the BMBF BioFung project. M.N. was supported by DFG grant NO407/5-1 and thanks Ulrich Kück and Christopher Grefen for support at Ruhr-Universität Bochum. Open-access funding enabled and organized by ProjektDEAL.

#### DATA AVAILABILITY STATEMENT

The genome data are deposited under the BioProject accession numbers PRJNA643983, PRJNA643984, and PRJNA643985. Many predicted transcripts did not pass the filters of NCBI during genome submission. Thus, the number of originally predicted transcripts (used for this study) and the number of submitted transcripts differs. We therefore provide genomes and the full set of predicted transcripts at [http://bioinf.uni-greifswald.de/bioinf/katharina/verticillium\\_full\\_data](http://bioinf.uni-greifswald.de/bioinf/katharina/verticillium_full_data)

#### ORCID

Bart P. H. J. Thomma  <https://orcid.org/0000-0003-4125-4181>

Gerhard H. Braus  <https://orcid.org/0000-0002-3117-5626>

#### REFERENCES

- Almagro Armenteros, J.J., Sønderby, C.K., Sønderby, S.K., Nielsen, H. & Winther, O. (2017) DeepLoc: prediction of protein subcellular localization using deep learning. *Bioinformatics*, **33**, 3387–3395.
- Bui, T.-T., Harting, R., Braus-Stromeier, S.A., Tran, V.-T., Leonard, M., Höfer, A. et al. (2019) *Verticillium dahliae* transcription factors Som1 and Vta3 control microsclerotia formation and sequential steps of plant root penetration and colonisation to induce disease. *New Phytologist*, **221**, 2138–2159.
- Caracul, Z., Roncero, M.I.G., Espeso, E.A., González-Verdejo, C.I., García-Maceira, F.I. & Di Pietro, A. (2003) The pH signalling transcription factor PacC controls virulence in the plant pathogen *Fusarium oxysporum*. *Molecular Microbiology*, **48**, 765–779.
- Casadevall, A. & Pirofski, L.-A. (2014) Microbiology: Ditch the term pathogen. *Nature*, **516**, 165–166.
- Casadevall, A. & Pirofski, L.-A. (2018) What is a host? Attributes of individual susceptibility. *Infection and Immunity*, **86**, 1–12.
- Chen, J.-Y., Liu, C., Gui, Y.-J., Si, K.-W., Zhang, D.-D., Wang, J. et al. (2018) Comparative genomics reveals cotton-specific virulence factors in flexible genomic regions in *Verticillium dahliae* and evidence of horizontal gene transfer from *Fusarium*. *New Phytologist*, **217**, 756–770.
- Cho, Y., Srivastava, A., Ohm, R.A., Lawrence, C.B., Wang, K.-H., Grigoriev, I.V. et al. (2012) Transcription factor Amr1 induces melanin biosynthesis and suppresses virulence in *Alternaria brassicicola*. *PLoS Pathogens*, **8**, 1002974.
- Clewes, E., Edwards, S.G. & Barbara, D.J. (2008) Direct molecular evidence supports long-spored microsclerotial isolates of *Verticillium* from crucifers being interspecific hybrids. *Plant Pathology*, **57**, 1047–1057.
- Coghlan, A., Eichler, E., Oliver, S., Paterson, A. & Stein, L. (2006) Chromosome evolution in eukaryotes: A multi-kingdom perspective. *Trends in Genetics*, **21**, 673–682.
- Cook, D.E., Kramer, M., Torres, D.E., Seidl, M.F. & Thomma, B.P.H.J. (2020) A unique chromatin profile defines adaptive genomic regions in a fungal plant pathogen. *eLife*, **9**, e62208.
- Coppin, E., de Renty, C. & Debuchy, R. (2005) The function of the coding sequences for the putative pheromone precursors in *Podospora anserina* is restricted to fertilization. *Eukaryotic Cell*, **4**, 407–420.
- Debuchy, R., Berteaux-Lecellier, V. & Silar, P. (2010) Mating systems and sexual morphogenesis in Ascomycetes. In: Borkovich, K. & Ebbole, D. (Eds.) *Cellular and molecular biology of filamentous fungi*. Washington, DC: American Society of Microbiology, pp. 501–535.
- Debuchy, R. & Turgeon, B.G. (2006) Mating-type structure, evolution, and function in Euscomycetes. In: Kües, U. & Fischer, R. (Eds.) *Growth, differentiation and sexuality*. Berlin/Heidelberg: Springer-Verlag, pp. 293–323.
- Depotter, J.R.L., Rodríguez-Moreno, L., Thomma, B.P.H.J. & Wood, T. (2017) The emerging British *Verticillium longisporum* population consists of aggressive *Brassica* pathogens. *Phytopathology*, **107**, 1399–1405.
- Depotter, J.R.L., Seidl, M.F., van den Berg, G.C.M., Thomma, B.P.H.J. & Wood, T.A. (2017) A distinct and genetically diverse lineage of the hybrid fungal pathogen *Verticillium longisporum* population causes stem striping in British oilseed rape. *Environmental Microbiology*, **19**, 3997–4009.
- Depotter, J.R.L., Seidl, M.F., Wood, T.A. & Thomma, B.P.H.J. (2016) Interspecific hybridization impacts host range and pathogenicity of filamentous microbes. *Current Opinion in Microbiology*, **32**, 7–13.
- Depotter, J.R.L., Shi-Kunne, X., Missonnier, H., Liu, T., Faino, L., van den Berg, G.C.M. et al. (2019) Dynamic virulence-related regions of the plant pathogenic fungus *Verticillium dahliae* display enhanced sequence conservation. *Molecular Ecology*, **28**, 3482–3495.
- Dong, S., Raffaele, S. & Kamoun, S. (2015) The two-speed genomes of filamentous pathogens: Waltz with plants. *Current Opinion in Genetics & Development*, **35**, 57–65.



- EFSA Panel on Plant Health, (PLH) (2014) Scientific opinion on the pest categorisation of *Verticillium dahliae* Kleb. *EFSA Journal*, 12, 3928.
- Eynck, C., Koopmann, B., Grunewaldt-Stoecker, G., Karlovsky, P. & von Tiedemann, A. (2007) Differential interactions of *Verticillium longisporum* and *V. dahliae* with *Brassica napus* detected with molecular and histological techniques. *European Journal of Plant Pathology*, 118, 259–274.
- Faino, L., Seidl, M.F., Datema, E., van den Berg, G.C.M., Janssen, A., Wittenberg, A.H.J. et al. (2015) Single-molecule real-time sequencing combined with optical mapping yields completely finished fungal genome. *mBio*, 6, e00936-15.
- Faino, L., Seidl, M.F., Shi-Kunne, X., Pauper, M., van den Berg, G.C.M., Wittenberg, A.H.J. et al. (2016) Transposons passively and actively contribute to evolution of the two-speed genome of a fungal pathogen. *Genome Research*, 26, 1091–1100.
- Fogelqvist, J., Tzelepis, G., Bejai, S., Ilbäck, J., Schwelm, A. & Dixelius, C. (2018) Analysis of the hybrid genomes of two field isolates of the soil-borne fungal species *Verticillium longisporum*. *BMC Genomics*, 19, 14.
- Fradin, E.F., Zhang, Z., Juarez Ayala, J.C., Castroverde, C.D.M., Nazar, R.N., Robb, J. et al. (2009) Genetic dissection of *Verticillium* wilt resistance mediated by tomato *Ve1*. *Plant Physiology*, 150, 320–332.
- Galazka, J.M. & Freitag, M. (2014) Variability of chromosome structure in pathogenic fungi – of “ends and odds”. *Current Opinion in Microbiology*, 20, 19–26.
- Gibriel, H.A.Y., Li, J., Zhu, L., Seidl, M.F. & Thomma, B.P.H.J. (2019) *Verticillium dahliae* strains that infect the same host plant display 2 highly divergent effector catalogs. *bioRxiv*, <https://doi.org/10.1101/528729> [preprint].
- Harting, R., Höfer, A., Tran, V.-T., Weinhold, L.-M., Barghahn, S., Schlüter, R. et al. (2020) The *Vta1* transcriptional regulator is required for microscleerotia melanization in *Verticillium dahliae*. *Fungal Biology*, 124, 490–500.
- Hartmann, F.E., Sánchez-Vallet, A., McDonald, B.A. & Croll, D. (2017) A fungal wheat pathogen evolved host specialization by extensive chromosomal rearrangements. *The ISME Journal*, 11, 1189–1204.
- Hastie, A.C. (1973) Hybridization of *Verticillium albo-atrum* and *Verticillium dahliae*. *Transactions of the British Mycological Society*, 60, 511–523.
- Hastie, A.C. (1989) The analysis of *Verticillium* strain relationship. In: Tjamos, E.C. & Beckman, C.H. (Eds) *Vascular wilt diseases of plants*. Vol. 28. Berlin, Heidelberg: Springer Berlin Heidelberg, pp. 315–323.
- Inderbitzin, P., Bostock, R.M., Davis, R.M., Usami, T., Platt, H.W. & Subbarao, K.V. (2011) Phylogenetics and taxonomy of the fungal vascular wilt pathogen *Verticillium*, with the descriptions of five new species. *PLoS One*, 6, e28341.
- Inderbitzin, P., Davis, R.M., Bostock, R.M. & Subbarao, K.V. (2011) The ascomycete *Verticillium longisporum* is a hybrid and a plant pathogen with an expanded host range. *PLoS One*, 6, e18260.
- Inderbitzin, P., Davis, R.M., Bostock, R.M. & Subbarao, K.V. (2013) Identification and differentiation of *Verticillium* species and *V. longisporum* lineages by simplex and multiplex PCR assays. *PLoS One*, 8, e65990.
- Jin, L., Chen, D., Liao, S., Zhang, Y.u., Yu, F., Wan, P. et al. (2019) Transcriptome analysis reveals downregulation of virulence-associated genes expression in a low virulence *Verticillium dahliae* strain. *Archives of Microbiology*, 201, 927–941.
- de Jonge, R., Bolton, M.D., Kombrink, A., van den Berg, G.C.M., Yadeta, K.A. & Thomma, B.P.H.J. (2013) Extensive chromosomal reshuffling drives evolution of virulence in an asexual pathogen. *Genome Research*, 23, 1271–1282.
- de Jonge, R., Peter van Esse, H., Maruthachalam, K., Bolton, M.D., Santhanam, P., Saber, M.K. et al. (2012) Tomato immune receptor *Ve1* recognizes effector of multiple fungal pathogens uncovered by genome and RNA sequencing. *Proceedings of the National Academy of Sciences of the United States of America*, 109, 5110–5115.
- Jurka, J., Kapitonov, V., Pavlicek, A., Klonowski, P., Kohany, O. & Walichewicz, J. (2005) Repbase update, a database of eukaryotic repetitive elements. *Cytogenetic and Genome Research*, 110, 462–467.
- Karapapa, V.K., Bainbridge, B.W. & Heale, J.B. (1997) Morphological and molecular characterization of *Verticillium longisporum* comb. nov., pathogenic to oilseed rape. *Mycological Research*, 101, 1281–1294.
- Kersey, P.J., Allen, J.E., Allot, A., Barba, M., Boddu, S., Bolt, B.J. et al. (2018) Ensembl genomes 2018: an integrated omics infrastructure for non-vertebrate species. *Nucleic Acids Research*, 46, D802–D808.
- Kim, H. & Borkovich, K.A. (2006) Pheromones are essential for male fertility and sufficient to direct chemotropic polarized growth of trichogynes during mating in *Neurospora crassa*. *Eukaryotic Cell*, 5, 544–554.
- Klosterman, S.J., Subbarao, K.V., Kang, S., Veronese, P., Gold, S.E., Thomma, B.P.H.J. et al. (2011) Comparative genomics yields insights into niche adaptation of plant vascular wilt pathogens. *PLoS Pathogens*, 7, e1002137.
- Kolar, M., Punt, P.J., van den Hondel, C.A.M.J.J. & Schwab, H. (1988) Transformation of *Penicillium chrysogenum* using dominant selection markers and expression of an *Escherichia coli lacZ* fusion gene. *Gene*, 62, 127–134.
- Kombrink, A., Rovenich, H., Shi-Kunne, X., Rojas-Padilla, E., van den Berg, G.C.M., Domazakis, E. et al. (2017) *Verticillium dahliae* LysM effectors differentially contribute to virulence on plant hosts. *Molecular Plant Pathology*, 18, 596–608.
- Kosugi, S., Hasebe, M., Tomita, M. & Yanagawa, H. (2009) Systematic identification of cell cycle-dependent yeast nucleocytoplasmic shuttling proteins by prediction of composite motifs. *Proceedings of the National Academy of Sciences of the United States of America*, 106, 10171–10176.
- Kuzmin, E., VanderSluis, B., Nguyen Ba, A.N., Wang, W., Koch, E.N., Usaj, M. et al. (2020) Exploring whole-genome duplicate gene retention with complex genetic interaction analysis. *Science*, 368, eaaz5667.
- Leonard, M., Kühn, A., Harting, R., Maurus, I., Nagel, A., Starke, J. et al. (2020) *Verticillium longisporum* elicits media-dependent secretome responses with capacity to distinguish between plant-related environments. *Frontiers in Microbiology*, 11, 1876.
- Mayrhofer, S., Weber, J.M. & Pöggeler, S. (2006) Pheromones and pheromone receptors are required for proper sexual development in the homothallic ascomycete *Sordaria macrospora*. *Genetics*, 172, 1521–1533.
- Metzenberg, R.L. & Glass, N.L. (1990) Mating type and mating strategies in *Neurospora*. *BioEssays*, 12, 53–59.
- Milgroom, M.G., Jiménez-Gasco, M.D.M., Olivares García, C., Drott, M.T. & Jiménez-Díaz, R.M. (2014) Recombination between clonal lineages of the asexual fungus *Verticillium dahliae* detected by genotyping by sequencing. *PLoS One*, 9, e106740.
- Mitchell, A.L., Attwood, T.K., Babbitt, P.C., Blum, M., Bork, P., Bridge, A. et al. (2019) InterPro in 2019: improving coverage, classification and access to protein sequence annotations. *Nucleic Acids Research*, 47, D351–D360.
- Möller, M. & Stukenbrock, E.H. (2017) Evolution and genome architecture in fungal plant pathogens. *Nature Reviews Microbiology*, 15, 756–771.
- Morales, L. & Dujon, B. (2012) Evolutionary role of interspecies hybridization and genetic exchanges in yeasts. *Microbiology and Molecular Biology Reviews*, 76, 721–739.
- Novakazi, F., Inderbitzin, P., Sandoya, G., Hayes, R.J., von Tiedemann, A. & Subbarao, K.V. (2015) The three lineages of the diploid hybrid *Verticillium longisporum* differ in virulence and pathogenicity. *Phytopathology*, 105, 662–673.
- Nowrousian, M., Stajich, J.E., Chu, M., Engh, I., Espagne, E., Halliday, K. et al. (2010) *De novo* assembly of a 40 Mb eukaryotic genome from short sequence reads: *Sordaria macrospora*, a model organism for fungal morphogenesis. *PLoS Genetics*, 6, e1000891.

- Nowrousian, M., Teichert, I., Masloff, S. & Kück, U. (2012) Whole-genome sequencing of *Sordaria macrospora* mutants identifies developmental genes. *G3, Genes, Genomes, Genetics*, 2, 261–270.
- Pantou, M.P. & Typas, M.A. (2005) Electrophoretic karyotype and gene mapping of the vascular wilt fungus *Verticillium dahliae*. *FEMS Microbiology Letters*, 245, 213–220.
- Pegg, G.F. & Brady, B.L. (2002) *Verticillium wilts*. Wallingford, UK: CAB International.
- Plissonneau, C., Hartmann, F. & Croll, D. (2018) Pangenome analyses of the wheat pathogen *Zymoseptoria tritici* reveal the structural basis of a highly plastic eukaryotic genome. *BMC Biology*, 16, 5.
- Pöggeler, S. (2001) Mating-type genes for classical strain improvements of Ascomycetes. *Applied Microbiology and Biotechnology*, 56, 589–601.
- Pöggeler, S. (2011) Function and evolution of pheromones and pheromone receptors in filamentous Ascomycetes. In: Pöggeler, S. and Wöstemeyer, J. (Eds.) *Evolution of fungi and fungal-like organisms (The Mycota)*. Heidelberg, New York: Springer, pp. 73–96.
- Potato Genome Sequencing Consortium (2011) Genome sequence and analysis of the tuber crop potato. *Nature*, 475, 189–195.
- Resende, M.L.V., Flood, J. & Cooper, R.M. (1994) Host specialization of *Verticillium dahliae*, with emphasis on isolates from cocoa (*Theobroma cacao*). *Plant Pathology*, 43, 104–111.
- Reusche, M., Thole, K., Janz, D., Truskina, J., Rindfleisch, S., Drübert, C. et al. (2012) *Verticillium* infection triggers VASCULAR-RELATED NAC DOMAIN7-dependent *de novo* xylem formation and enhances drought tolerance in *Arabidopsis*. *The Plant Cell*, 24, 3823–3837.
- Rouxel, T., Grandaubert, J., Hane, J.K., Hoede, C., van de Wouw, A.P., Couloux, A. et al. (2011) Effector diversification within compartments of the *Leptosphaeria maculans* genome affected by repeat-induced point mutations. *Nature Communications*, 2, 202.
- Santhanam, P. & Thomma, B.P.H.J. (2013) *Verticillium dahliae* Sge1 differentially regulates expression of candidate effector genes. *Molecular Plant-Microbe Interactions*, 26, 249–256.
- Schmoll, M., Seibel, C., Tisch, D., Dorrer, M. & Kubicek, C.P. (2010) A novel class of peptide pheromone precursors in ascomycetous fungi. *Molecular Microbiology*, 77, 1483–1501.
- Seidl, M.F., Kramer, H.M., Cook, D.E., Fiorin, G.L., van den Berg, G.C.M., Faino, L. et al. (2020) Repetitive elements contribute to the diversity and evolution of centromeres in the fungal genus *Verticillium*. *mBio*, 11, e01714–20.
- Seidl, M.F. & Thomma, B.P.H.J. (2014) Sex or no sex: evolutionary adaptation occurs regardless. *BioEssays*, 36, 335–345.
- Seidl, M.F. & Thomma, B.P.H.J. (2017) Transposable elements direct the coevolution between plants and microbes. *Trends in Genetics*, 33, 842–851.
- Selin, C., de Kievit, T.R., Belmonte, M.F. & Fernando, W.G.D. (2016) Elucidating the role of effectors in plant-fungal interactions: Progress and challenges. *Frontiers in Microbiology*, 7, 600.
- Sharma, R., Mishra, B., Runge, F. & Thines, M. (2014) Gene loss rather than gene gain is associated with a host jump from monocots to dicots in the smut fungus *Melanopsichium pennsylvanicum*. *Genome Biology and Evolution*, 6, 2034–2049.
- Shi-Kunne, X., Faino, L., van den Berg, G.C.M., Thomma, B.P.H.J. & Seidl, M.F. (2018) Evolution within the fungal genus *Verticillium* is characterized by chromosomal rearrangement and gene loss. *Environmental Microbiology*, 20, 1362–1373.
- Short, D.P.G., Gurung, S., Hu, X., Inderbitzin, P. & Subbarao, K.V. (2014) Maintenance of sex-related genes and the co-occurrence of both mating types in *Verticillium dahliae*. *PLoS One*, 9, e112145.
- Singh, S., Braus-Stromeier, S.A., Timpner, C., Tran, V.T., Lohaus, G., Reusche, M. et al. (2010) Silencing of *Vlora2* for chorismate synthase revealed that the phytopathogen *Verticillium longisporum* induces the cross-pathway control in the xylem. *Applied Microbiology and Biotechnology*, 85, 1961–1976.
- Slater, G.S.C. & Birney, E. (2005) Automated generation of heuristics for biological sequence comparison. *BMC Bioinformatics*, 6, 31.
- Stanke, M., Diekhans, M., Baertsch, R. & Haussler, D. (2008) Using native and syntenically mapped cDNA alignments to improve *de novo* gene finding. *Bioinformatics*, 24, 637–644.
- Steenwyk, J.L., Lind, A.L., Ries, L.N.A., dos Reis, T.F., Silva, L.P., Almeida, F. et al. (2020) Pathogenic allopolyploid hybrids of *Aspergillus* fungi. *Current Biology*, 30, 2495–2507.
- Stergiopoulos, I. & de Wit, P.J.G.M. (2009) Fungal effector proteins. *Annual Review of Phytopathology*, 47, 233–263.
- Stukenbrock, E.H., Christiansen, F.B., Hansen, T.T., Dutheil, J.Y. & Schierup, M.H. (2012) Fusion of two divergent fungal individuals led to the recent emergence of a unique widespread pathogen species. *Proceedings of the National Academy of Sciences of the United States of America*, 109, 10954–10959.
- Tang, Y.-C. & Amon, A. (2013) Gene copy-number alterations: a cost-benefit analysis. *Cell*, 152, 394–405.
- Teichert, I., Wolff, G., Kück, U. & Nowrousian, M. (2012) Combining laser microdissection and RNA-seq to chart the transcriptional landscape of fungal development. *BMC Genomics*, 13, 511.
- Traeger, S., Altegoer, F., Freitag, M., Gabaldon, T., Kempken, F., Kumar, A. et al. (2013) The genome and development-dependent transcriptomes of *Pyronema confluens*: a window into fungal evolution. *PLoS Genetics*, 9, e1003820.
- Tran, V.-T., Braus-Stromeier, S.A., Kusch, H., Reusche, M., Kaefer, A., Kühn, A. et al. (2014) *Verticillium* transcription activator of adhesion Vta2 suppresses microsclerotia formation and is required for systemic infection of plant roots. *New Phytologist*, 202, 565–581.
- Tran, V.-T., Braus-Stromeier, S.A., Timpner, C. & Braus, G.H. (2013) Molecular diagnosis to discriminate pathogen and apathogen species of the hybrid *Verticillium longisporum* on the oilseed crop *Brassica napus*. *Applied Microbiology and Biotechnology*, 97, 4467–4483.
- Turgeon, B.G. & Yoder, O.C. (2000) Proposed nomenclature for mating type genes of filamentous ascomycetes. *Fungal Genetics and Biology*, 31, 1–5.
- Validov, S.Z., Kamilova, F.D. & Lugtenberg, B.J.J. (2011) Monitoring of pathogenic and non-pathogenic *Fusarium oxysporum* strains during tomato plant infection. *Microbial Biotechnology*, 4, 82–88.
- Wang, Y., Hu, X., Fang, Y., Anchieta, A., Goldman, P.H., Hernandez, G. et al. (2018) Transcription factor VdCmr1 is required for pigment production, protection from UV irradiation, and regulates expression of melanin biosynthetic genes in *Verticillium dahliae*. *Microbiology*, 164, 685–696.
- Zeise, K. & von Tiedemann, A. (2002) Host specialization among vegetative compatibility groups of *Verticillium dahliae* in relation to *Verticillium longisporum*. *Journal of Phytopathology*, 150, 112–119.
- Zerbino, D.R. & Birney, E. (2008) Velvet: algorithms for *de novo* short read assembly using de Bruijn graphs. *Genome Research*, 18, 821–829.
- Zhou, L., Hu, Q., Johansson, A. & Dixelius, C. (2006) *Verticillium longisporum* and *V. dahliae*: infection and disease in *Brassica napus*. *Plant Pathology*, 55, 137–144.

## SUPPORTING INFORMATION

Additional Supporting Information may be found online in the Supporting Information section.

**How to cite this article:** Harting R, Starke J, Kusch H, et al. A 20-kb lineage-specific genomic region tames virulence in pathogenic amphidiploid *Verticillium longisporum*. *Mol Plant Pathol*. 2021;22:939–953. <https://doi.org/10.1111/mpp.13071>